J Mater Sci (2010) 45:5406–5411
DOI 10.1007/s10853-010-4593-2

Effects of concentration on the alkali-treatment of ZSM-5 zeolite: a study on dividing points

Liang Zhao · Chunming Xu · Shan Gao · Baojian Shen

Received: 23 December 2009 / Accepted: 4 May 2010 / Published online: 19 May 2010

Abstract Alkali-treatment for modification or dissolution has attracted extensive attention as an innovative means of preparing porous materials. The hierarchical porosity of modified zeolite is highly dependent on its treatment conditions. However, studies on critical alkali-treatment concentrations, specifically those that discuss the dividing points, have not yet been reported. In this article, the pore and crystalline properties of ZSM-5 zeolite samples modified by different concentrations of alkali-treatment are investigated. The experimental results show that the pore properties of the samples change as a function of the alkaline concentration. The total surface, mesopore surface area, total pore volume, mesopore volume, and average pore diameter of ZSM-5 zeolites increase and then decrease with increasing alkaline concentrations. The micropore surface area, micropore volume, and crystallinity of the samples decrease monotonously. The following dividing points are proposed: 0.40 mol/L as the threshold for alkali-modification and 1.00 mol/L as the starting point for alkali-dissolution. A possible desilication mechanism is also proposed.

Introduction

Alkali-treatment has attracted extensive attention as an innovative post-treatment method and is regarded as a promising approach for the preparation of porous materials [1–10]. Generally, alkali-treatment involves alkali-dissolution and alkali-modification, depending on the solution concentration used. The solution concentration required for alkali-dissolution is usually higher than that for alkali-modification.

The two alkali-treatments, dissolution and modification, have different purposes in zeolite preparation. Alkali-modification utilizes low concentrations of the solution to treat zeolite samples with the aim of selectively removing silicon species and preserving the micropores. Ideal hierarchical zeolites are then expected to be obtained. Pérez-Ramírez et al. [11] pointed out that hierarchical zeolites should possess the attributes of mesoporous networks, such as high accessibility, transportability, and catalytic selectivity. Fortunately, the co-existence of micropores and mesopores can be achieved in a single zeolite by means of controlled alkali-modification in low-concentration solutions [1, 3, 7, 12–14]. Improved catalytic performance and enhanced active site accessibility has been reported [15–19] to originate from the beneficial effects of faster reactant and product diffusion rates. High levels of selectivity are also maintained in preserved microporous systems.

Such hierarchical structures, however, can be destroyed if the concentration of the alkali solution exceeds a certain level. When this occurs, the zeolite framework is loosened or destroyed, and smaller units of zeolite structures are obtained. This is what happens during the so-called alkali-dissolution. By means of alkali-dissolution, Inagaki et al. [20], Zhang et al. [21], and Song et al. [22, 23] were able to successfully synthesize strong B-acid MCM-41 zeolites with active aluminum silicon pieces extracted from ZSM-5 zeolite. Other studies in this field have been performed, an example of which is one led by Čižmek et al. [24, 25] who investigated the dissolution behavior of silicalite-1 and

Electronic supplementary material The online version of this article (doi:10.1007/s10853-010-4593-2) contains supplementary material, which is available to authorized users.

L. Zhao · C. Xu · S. Gao · B. Shen (✉)
State Key Laboratory of Heavy Oil Processing, China University of Petroleum, 102249 Beijing, China
e-mail: baojian@cup.edu.cn

ZSM-5 at 333 K and in 5 M NaOH solution. The results of such a study allowed for the derivation of the dissolution kinetics equation for silicate-1-dissolving processes in alkali solutions.

The essential difference between the two treatments is the concentration of the alkali solutions used, specifically called the dividing point. Although some investigations on dissolution and modification have been conducted in the past, studies that discuss the dividing point are rare. To the best of our knowledge, no literature has yet been published on the dividing point of alkali solutions.

In this study, variations in the porous properties and crystallinities of ZSM-5 zeolite samples with an SiO_2/Al_2O_3 ratio of 38 were investigated under the following reaction conditions: a reaction temperature of 363 K, a reaction time of 300 min, and varying alkali concentrations ranging from 0.10 to 2.00 M. Investigation on the dividing points of alkali-treatments will give detailed information on the changes in the properties of ZSM-5 zeolites. Such knowledge will be helpful for selecting treatment conditions for different applications.

Experimental details

Commercially available NaZSM-5 zeolites with an SiO_2/Al_2O_3 ratio of 38 (Beijing Balvin-Kalvin Co. Ltd) were used as raw materials. NaZSM-5 zeolites were alkali-treated as per the following procedure. First, approximately 10.0 g of NaZSM-5 zeolite were immersed in 300 mL of an aqueous NaOH solution with different concentrations and then stirred for 300 min at 363 K. Afterward, the slurry was cooled rapidly in an ice bath, filtered, and washed with distilled water until a neutral filtrate pH was obtained. The remaining solid was dried in air for 4 h at 363 K. After drying, the alkali-treated NaZSM-5 was ion-exchanged with a 0.4 M $(NH_4)_2SO_4$ aqueous solution and stirred for 60 min at 363 K, followed by filtration and rinsing with distilled water to remove excess sodium ions. This procedure was repeated twice to obtain NH_4ZSM-5. After drying overnight at 393 K, NH_4ZSM-5 was then calcined in static air for 4 h at 813 K to form HZSM-5 samples.

X-ray diffraction (XRD) patterns were measured using a Shimadzu-6000 diffractometer with a CuKα radiation at 40 mA and 40 mV. The samples were scanned at a rate of 4°/min in the range of 5° to 50° to confirm the structure of ZSM-5 and at a rate of 0.5°/min in the range of 22.5° to 25° to identify characteristic peaks of ZSM-5 zeolites. The relative crystallinity was estimated by calculating the peak area in the 2θ range of 22.5°–25° using Eq. 1:

$$\alpha = \alpha_0 \times I/I_0, \quad (1)$$

where α (%) and α_0 (%) are the crystallinities of the unknown and standard samples, respectively; and I and I_0 are the integration areas of the specific diffraction peaks of the unknown and standard samples, respectively.

The N_2-adsorption/desorption isotherms were recorded on a Quantachrome Autosorb Automated Gas Sorption analyzer at 77 K. The total surface area was calculated according to the BET isothermal equation. The micropore volume, mesopore volume, and external surface area were evaluated using a *t*-plot method. The pore size was reported as the average pore diameter.

Results and discussion

In order to investigate the effects of concentration on the pore structure properties of ZSM-5 zeolites, the experiments were performed under a constant reaction temperature of 363 K, stirring time of 300 min, and increasing concentrations of NaOH in the range of 0.10–2.00 M. Table 1 shows the porosity properties of ZSM-5 zeolites prepared from alkali-treatment with various concentrations. The samples were numbered from 01 to 11 with increasing NaOH concentration. The raw material zeolite was numbered 00 (Sample 00) and used as a reference. In order to categorize hierarchical porous zeolites, the hierarchical factors (HFs) [26] were calculated. The HF of ZSM-5 zeolites was determined as the product of $(V_{micro}/V_p) \times (S_{meso}/S_{BET})$. In this article, the yield is defined as the ratio between the mass of treated samples and the initial mass of each sample.

Mesopores and macropores can be introduced into ZSM-5 zeolites during alkali-treatment. Samples 02 and 09 were selected at random to represent different levels of alkali-treatment. The adsorption–desorption isotherms and the pore diameter distributions of the ZSM-5 zeolites before and after alkali-treatment are shown in Fig. 1a, b.

The original ZSM-5 zeolite (Sample 00) has a Type-I isotherm with a plateau at relatively higher pressures and no distinct hysteresis loop. This is a typical isotherm for microporous materials. As can be seen in Fig. 1b, majority of pores in Sample 00 are micropores. The pore-size distribution is broad for diameters smaller than 2 nm, and the distribution curve shows a small peak at around 3.5 nm. There are hardly any peaks after 4 nm. Through *t*-plot measurements, the average pore diameter was found to be 2.24 nm.

After alkali-modification, ZSM-5 Sample 02 shows a typical Type-IV isotherm. The zeolitic structure has a remarkably enhanced N_2 adsorption capacity accompanied by a hysteresis loop, indicative of extra mesoporosity. The shape of the hysteresis loop implies that mesopores

Table 1 The porosity properties of ZSM-5 zeolite prepared from alkali-treatment

Code	C_{NaOH} (mol/L)	D_{aver} (nm)	S_{BET} (m^2/g)	$S_{total\text{-}micro}$ (m^2/g)	$S_{micropore}$ (m^2/g)	V_p (cm^3/g)	V_{micro} (cm^3/g)	$V_{p\text{-}micro}$ (cm^3/g)	HF	Yield (%)
00	–	2.24	380	22	358	0.212	0.171	0.042	0.0467	–
01	0.10	2.69	384	62	322	0.258	0.159	0.099	0.0995	84.0
02	0.15	3.15	396	101	295	0.312	0.150	0.162	0.1226	76.5
03	0.20	3.45	414	131	283	0.357	0.144	0.213	0.1276	72.2
04	0.25	3.80	395	149	246	0.375	0.131	0.244	0.1318	67.1
05	0.30	5.04	396	220	176	0.499	0.092	0.407	0.1024	55.5
06	0.35	5.85	390	249	141	0.571	0.072	0.499	0.0805	51.5
07	0.40	6.50	368	258	110	0.598	0.055	0.543	0.0645	50.3
08	0.50	7.95	258	225	33	0.513	0.018	0.495	0.0306	38.7
09	0.80	9.40	84	66	18	0.499	0.009	0.490	0.0142	27.6
10	1.00	17.27	72	72	0	0.311	0	0.311	0.0000	19.3
11	1.20	16.38	70	52	18	0.315	0.008	0.307	0.0189	13.8
12	1.50	15.26	77	77	0	0.294	0	0.294	0.0000	11.0
13	2.00	10.05	62	47	15	0.158	0.006	0.152	0.0288	4.8

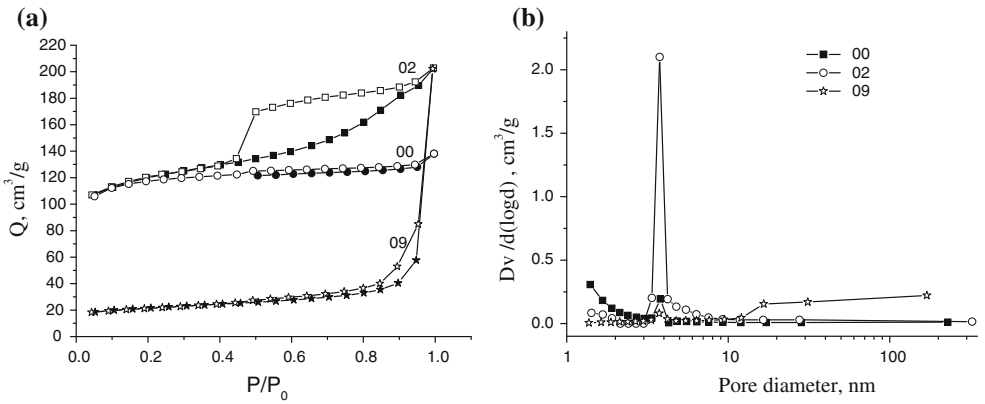

Fig. 1 **a** N_2-adsorption and desorption isotherms at 77 K of ZSM-5 zeolite before and after alkali-treatment; **b** corresponding BJH pore-size distribution of ZSM-5 zeolite before and after alkali-treatment

exist in the zeolite. The total adsorption capacity of Sample 02 is much larger than that of Sample 00. The pore distribution curve of Sample 02 emerges as a sharp peak at around 3.8 nm, and the height of the sharp peak is almost 10-fold that of the peak at 3.5 nm in the curve of Sample 00. Compared to Sample 00, the quantity of micropores in Sample 02 modified by alkali is slightly lower, and the pore diameter distribution after 4.0 nm is broadly distributed. After *t*-plot measurements, the average pore diameter was found to be 3.15 nm. Groen et al. [27] pointed out that a forced closure of the hysteresis loop around P/P_0 0.42 in the case of N_2 at 77 K could cause an erroneous assignment of this phenomenon to the presence of physical pores around 4 nm. The group believed that the BJH model may have limitations with regard to the traditionally called tensile strength effect of the adsorbed phase. As such, we cannot confirm that the peak at 3.8 nm represents real physical pores using only this characterization method. However, the large variation in N_2 adsorption capacities, specifically $Dv/d(\log d)$, indicated that more pores (including mesopores and other pores formed among the ZSM-5 particles) exist in Sample 02 than in Sample 00.

ZSM-5 Sample 09 shows a markedly different isotherm compared to the two other samples. The shape of Sample 09's isotherm is similar to a Type-I isotherm but with a lower adsorption ability. After a P/P_0 of 0.9, the adsorption isotherm rapidly increases, indicating a high-adsorption capability equal to that of Sample 02. This suggests that the internal pore system of the zeolite is destroyed and that capillary condensation occurs on the surface and intracrystalline portions of zeolite. Based on the pore-size distributions, the following observations can be made: (1) no pores exist that are smaller than 2 nm in diameter, (2) a very small peak occurs at around 3.8 nm, and (3) a broad

distribution appears beyond the 15 nm pore size. These results show that the zeolite framework collapsed and that the micropore system was destroyed.

Alkali-treatments using various solution concentrations led to different ZSM-5 zeolite porosity properties. Figure 2 shows the trends in the zeolite BET total surface area (S_{BET}), mesopore surface area ($S_{total\text{-}micro}$), and micropore surface area (S_{micro}) with varying solution concentrations of NaOH.

Results reveal that the S_{BET} of zeolite slightly varies with NaOH concentrations between 0.10 and 0.40 M. It then decreases rapidly until a concentration of 1.00 M. Beyond this concentration, the S_{BET} remains almost constant. The $S_{total\text{-}micro}$ gradually increases with increasing NaOH concentrations in the range of 0.10–0.40 M, reaching a maximum value (258 cm^3/g) at 0.40 M. It then showed the same trend as S_{BET} in the concentration range of 0.40–2.00 M. The S_{micro} also decreases with increasing NaOH concentrations and reaches zero after 1.00 M. This indicates that the microporous structure of zeolite collapses due to the rupture of Si–O bonds during treatment.

This research work also focuses on changes in the pore volume properties of zeolite with varying NaOH solution concentrations. The volume properties investigated include the total pore volume (V_p), mesopore volume ($V_{p\text{-}micro}$), and micropore volume (V_{micro}) of zeolites. Both V_p and the $V_{p\text{-}micro}$ increase with increasing NaOH solution concentrations. They attain their maximum volume at 0.40 M (Fig. 3). From the concentrations 0.40–2.00 M, the volumes decline with increasing basicity. The V_{micro} of zeolite decreases with increasing NaOH concentrations. The results suggest that silicon species on the framework of the microstructures partly dissolve and that mesopores are formed on the surface of or within the zeolite structures when the alkali concentration is lower than 0.40 M. Due to the formation of mesopores, the V_p and the $V_{p\text{-}micro}$ gradually increases. Nevertheless, with rigorous treatment, more silicon species are dissolved and the zeolite structure becomes extensively destroyed. This ultimately leads to a loss of micropores.

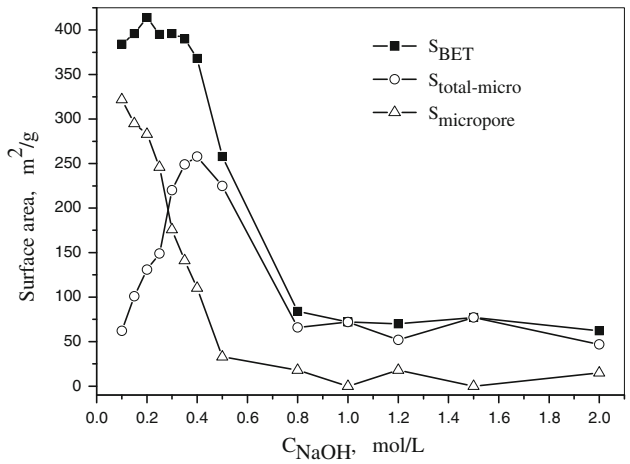

Fig. 2 The variation curve of surface area of ZSM-5 zeolite with the concentration of NaOH

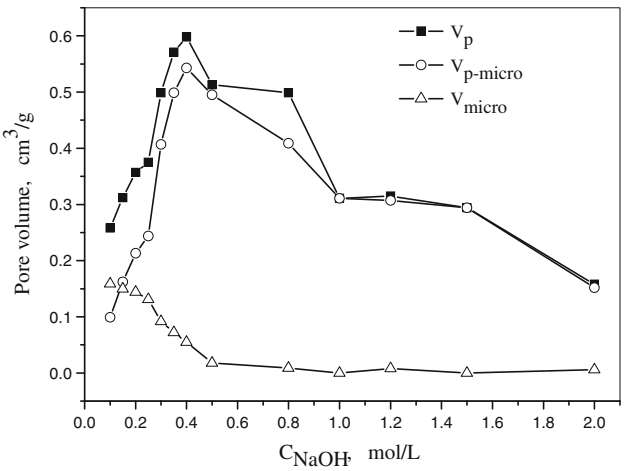

Fig. 3 The variation curve of pore volume of ZSM-5 zeolite with the concentration of NaOH

Figure 4 shows the average pore diameter and crystallinity of zeolite versus the concentration of NaOH. The average pore diameter steadily increases in the concentration range of 0.10–1.00 M. This is because the silicon species are removed from the zeolite framework, thus allowing the formation of mesopores and macropores in the pore system. However, the pore diameter gradually decreases after treatment with alkali concentrations of 1.00 M. This indicates that the zeolite structure collapses because of the treatment.

The XRD patterns shown in Fig. 5 also confirm the changes to the zeolite structures with increasing alkali concentrations. Normally, the peaks in the range of 6°–9° and 22.5°–25° are the characteristics peaks of ZSM-5

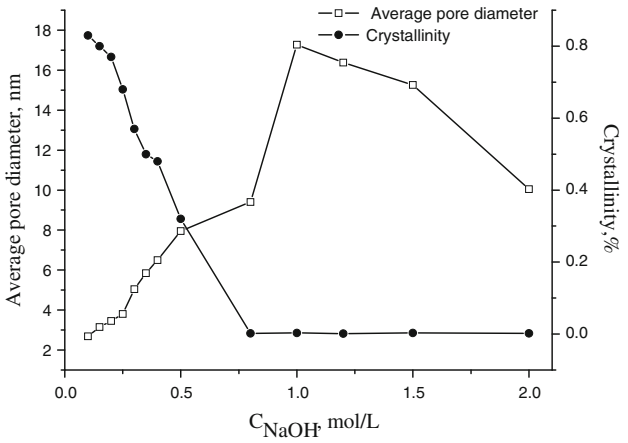

Fig. 4 The variation curve of average pore diameter (*open square*) and the crystallinity (*closed circle*) of ZSM-5 zeolite with the concentration of NaOH

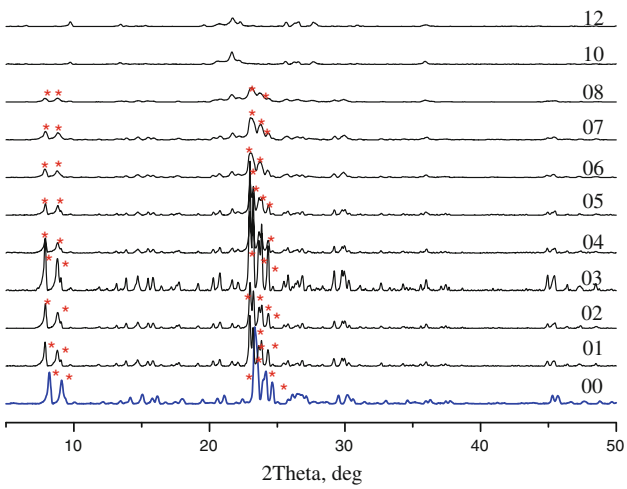

Fig. 5 XRD pattern of ZSM-5 zeolite under different alkali-treatment concentration. *Characteristic peaks of ZSM-5 zeolite, 2θ in the range of 6–9° and 22.5–25°. The standard XRD pattern of ZSM-5 zeolite is shown in Supporting Information ST1

(Supporting Information S1). The XRD pattern of Sample 00 shows all the characteristics peaks (marked by stars) of a standard ZSM-5 zeolite. From Sample 01 to 04, the intensities of the characteristic peaks increase because the amorphous components are removed from the zeolite structure. However, the intensities of the peaks decrease with increasing alkali concentrations. The ZSM-5 zeolite has an amorphous structure when the alkali-treatment concentration exceeds 1.00 M. This is confirmed by the crystallinity data shown in Fig. 4. The crystallinity of zeolite decreases with increasing alkali concentration. Above concentrations of 1.0 M, the crystallinity of zeolite disappears, indicating that the alkali-treatment damages the framework structure and extracts smaller units of zeolite.

The HF [26] is applied as a powerful tool to categorize hierarchical porous zeolites, independent of the type and synthesis method used. In general, standard specimens that are mostly microporous in nature have moderate $HF \leq 0.1$. In extreme cases, largely mesoporous structures have $HF < 0.05$. High relative microporosity and low relative mesoporosity are associated with $HF > 0.10$. Zeolite samples that display largely spreading hierarchical systems are found to have $HF > 0.15$. In the current study, as shown in Table 1, the HF values of Samples 01, 02, 03, 04, and 05 are all greater than 0.10, indicating that these samples have high microporosity and low mesoporosity. The HF values for Samples 08 and 09 are less than 0.05, indicating that largely mesoporous structures formed. These data further prove that an alkali concentration of 0.4 M is the maximum concentration for mesopore production and that an alkali concentration of 1.0 M is the starting point for zeolite structure dissolution.

Yields were also calculated in this study. As shown in Table 1, the alkali-treated zeolite yields decrease monotonously with increasing alkali concentrations. This is likely due to the removal of increasing amounts of silicon and the resulting decrease in the residual solid mass of zeolite in increasingly basic solutions.

According to the above discussion, a desilication mechanism could be proposed. The initial formation of mesopores was started by removal of Si atom from crystals surface. With the increase of alkali concentration, silicon species in the zeolites framework began to be dissolved selectively, mesopores and macropores were introduced into zeolites. With further desilication to the intracrystalline of zeolites, the framework of zeolite was dissolved and structure units of zeolite were extracted.

Conclusions

In summary, the concentration of an alkali solution has significant effects on the zeolite pore properties and zeolite crystallinity. Mesopores can be introduced into the pore system of zeolites under the proper alkali concentrations. However, the structure of zeolite is entirely damaged if rigorous alkali concentration conditions are applied. Crystallinity is inversely proportional to the alkali concentration, while the surface area and pore volume of the zeolite exists as a maximum value. The pore size and pore distribution change with different concentrations of alkali solutions. Combining the mentioned results and HF discussion, the following dividing points are proposed: 0.4 M as the threshold for alkali-modification and 1.0 M as the starting point for alkali-dissolution. As the properties of zeolite are dependent on the SiO_2/Al_2O_3 ratio, the proposed dividing points are suitable for ZSM-5 samples with SiO_2/Al_2O_3 ratios of around 38. With increasing SiO_2/Al_2O_3 ratio, the dividing points should be increased accordingly. A simple desilication mechanism was proposed. ZSM-5 zeolites with different pore properties can be prepared by alkali-treatment and may be used for various catalytic reactions. As such, further studies should be made on the alkali-treatment of zeolites.

Acknowledgments The authors acknowledge the supports by the National Natural Science Foundation of China (Grant Nos. 20725620 and 20906102).

References

1. Groen JC, Bach T, Ziese U, Paulaime-van Donk AM, de Jong Krijn P, Moulijn JA, Pérez-Ramírez J (2005) J Am Chem Soc 127:10792

2. Le Van Mao R, Le ST, Ohayon D, Caillibot F, Gelebart L, Denes G (1997) Zeolites 19:270
3. Groen JC, Moulijn JA, Pérez-Ramírez J (2007) Ind Eng Chem Res 46:4193
4. Groen JC, Peffer LAA, Moulijn JA, Pérez-Ramírez J (2004) Micropor Mesopor Mater 69:29
5. Su LL, Liu L, Zhuang JQ, Wang HX, Li YG, Shen WJ, Xu Y, Bao XH (2003) Catal Lett 91:155
6. Groen JC, Jansen JC, Moulijn JA, Pérez-Ramírez J (2004) J Phys Chem B 108:13062
7. Groen JC, Moulijn JA, Pérez-Ramírez J (2006) J Mater Chem 16:2121
8. Panagiotopoulou C, Kontori E, Perraki T, Kakali G (2007) J Mater Sci 42:2967. doi:10.1007/s10853-006-0531-8
9. MacKenzie KJD, Brew DRM, Fletcher RA, Vagana R (2007) J Mater Sci 42:4667. doi:10.1007/s10853-006-0173-x
10. Nath DCD, Bandyopadhyay S, Yu AB, Blackburn D, White C (2010) J Mater Sci 45:1354. doi:10.1007/s10853-009-4091-6
11. Pérez-Ramírez J, Christensen CH, Egeblad K, Christensen CH, Groen JC (2008) Chem Soc Rev 37:2530
12. Ogura M, Shinomiya S, Tateno J, Nara Y, Nomura M, Kikuchi E, Matsukata M (2001) Appl Catal A Gen 219:33
13. Suzuki T, Okuhara T (2001) Micropor Mesopor Mater 43:83
14. Groen JC, Peffer LAA, Moulijin JA, Pérez-Ramírez J (2004) Colloids Surf A Physicochem Eng Aspects 241:53
15. Zhao L, Shen BJ, Gao JS, Xu CM (2008) J Catal 258:228
16. Groen JC, Zhu W, Brouwer S, Huynink SJ, Kapteijn F, Moulijn JA, Pérez-Ramírez J (2007) J Am Chem Soc 129:355
17. Jin F, Tian Y, Li YD (2009) Ind Eng Chem Res 48:1873
18. Bjørgen M, Joensen F, Holm MS, Olsbye U, Lillerud KP, Svelle S (2008) Appl Catal A Gen 345:43
19. Jung JS, Park JW, Seo G (2005) Appl Catal A 288:149
20. Inagaki S, Ogura M, Inami T, Sasaki Y, Kikuchi E, Matsukata M (2004) Micropor Mesopor Mater 74:163
21. Zhang Y, Dou T, Li YP, Shi DX, Zhao Z (2005) J Inorg Mater 20:1423
22. Song CM, Jiang J, Yan ZF (2008) J Porous Mater 15:205
23. Song CM, Yan ZF (2008) Asia-Pac J Chem Eng 3:275
24. Čižmek A, Subotić B, Aiello R, Crea F, Nastro A, Tuoto C (1995) Micropor Mater 43:159
25. Čižmek A, Subotić B, Šmit I, Tonejc A, Aiello R, Crea F, Nastro A (1997) Micropor Mater 8:159
26. Pérez-Ramírez J, Verboekend D, Bonilla A, Abello S (2009) Adv Funct Mater 19:3972
27. Groen JC, Pérez-Ramírez J (2004) Appl Catal A Gen 268:121